J. Chem. Sci., Vol. 122, No. 4, July 2010, pp. 621–630.

Catalytic synthesis of 2-methylpyrazine over Cr-promoted copper based catalyst via a cyclo-dehydrogenation reaction route

FANGLI JING, YUANYUAN ZHANG, SHIZHONG LUO*, WEI CHU*, HUI ZHANG and XINYU SHI

Department of Chemical Engineering, Sichuan University, NO. 24 South Section 1, Yihuan Road, Chengdu 610065, China
e-mail: luoszscu@gmail.com, chuwei65@yahoo.com.cn

MS received 14 May 2009; revised 4 October 2009; accepted 15 October 2009

Abstract. The cyclo-dehydrogenation of ethylene diamine and propylene glycol to 2-methylpyrazine was performed under the atmospheric conditions at 380°C. The Cr-promoted Cu-Zn/Al_2O_3 catalysts were prepared by impregnation method and characterized by ICP-AES, N_2 adsorption/desorption, XRD, XPS, N_2O chemisorption, TPR and NH_3-TPD techniques. The amorphous chromium species existing in Cu-Zn-Cr/Al_2O_3 catalyst enhanced the dispersion of active component Cu, promoted the reduction of catalyst. Furthermore, the catalytic performance was significantly improved. The acidity of the catalyst played an important role in increasing the 2-MP selectivity. To optimize the reaction parameters, influences of different chromium content, reaction temperature, liquid hourly space velocity (LHSV), reactants molar ratio and time on stream on the product pattern were studied. The results demonstrated that addition of chromium promoter revealed satisfying catalytic activity, stability and selectivity of 2-methylpyrazine.

Keywords. 2-Methylprazine; copper-based catalyst; chromium-promoter; ethylene diamine; propylene glycol; characterization.

1. Introduction

Pyrazine and its derivatives are valuable compounds because of their application in the synthesis of perfumery, pharmaceutical and agricultural chemical industries.[1–3] As an example, 2-methylpyrazine (2-MP), an important lower alkyl-substituted pyrazine, is widely used as a key intermediate for pyrazineamide, an effective anti-tubercular drug.[4,5] Currently, 2-methylpyrazine is prepared by dehydration-cyclization and/or partial dehydrogenation of ethylene diamine (ED) and propylene glycol (PG).[6] Forni and Pollesel[7] studied the mechanism of the cyclization of ethylene diamine and propylene glycol to 2-methylpyrazine by means of the TPD-TPR-MS technique. They pointed out that the reaction involves a Rideal–Eley mechanism leading to a fully hydrogenated intermediate 2-methylpiperazine between adsorbed propylene glycol and gaseous ethylene diamine. The mechanism is shown in scheme 1. Catalytic systems based on zinc,[8] zinc-chromium,[9] copper-chromium[10] and Ag[11] were patented. Other catalysts such as ZnO-MoO_3, ZnO-V_2O_5, Zn-WO_3,[12] ZnO-$MnSO_4$–H_3PO_4,[13] Ag-La-Zn/Al_2O_3, Ag-Pt/Al_2O_3, and Ag-Mg/Al_2O_3,[14] Pd-promoted ZnO/Zn-Cr-O catalysts,[15] zinc-modified ferrierite (FER),[16] H-ZSM-5, zinc-modified zeolite catalysts (including ZSM-5 and Beta)[17] were also used for synthesis of 2-methylpyrazine.

The catalysts containing chromium were extensively used for dehydrogenation of piperazine to pyrazine,[18,19] which indicated that catalysts containing chromium promoted effectively on the dehydrogenation reaction. Park *et al*[20,21] reported that metal (copper, nickel, cobalt) oxide-modified ZnO/SiO_2 for cyclo-dehydrogenation of ethylene diamine with propylene glycol to 2-methylpyrazine, demonstrated that the metallic copper and zinc oxide were assigned to dehydrogenation and dehydration, respectively. Since the catalytic synthesis of 2-methylpyrazine is related with cyclization (dehydration) and dehydrogenation of piperazine intermediate, the catalysts which should possess dual functional active sites, they have been designed,

*For correspondence

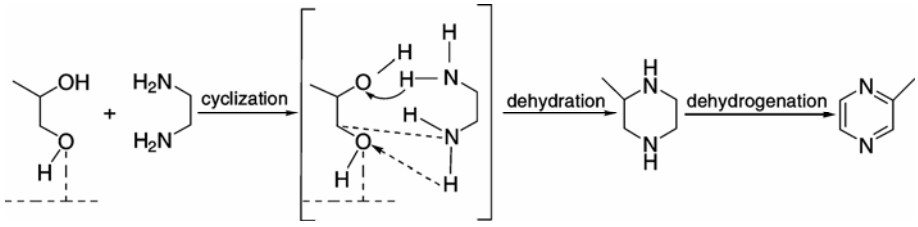

Scheme 1. Reaction pathway for the synthesis of 2-methylpyrazine from ethylene diamine and propylene glycol.

prepared and measured for 2-methylpyrazine synthesis.

In this work, a novel type bifunctional Cr-promoted Cu-Zn/Al_2O_3 oxide catalyst was proposed, characterized using inductively coupled plasma-atomic emission spectrometry (ICP-AES), X-ray diffraction (XRD), X-ray photoelectron spectra (XPS), N_2O chemisorption, etc. methods, to understand the chemical composition, the structure, the chemical state of elements and Cu surface area and dispersion of the catalyst and correlated these physicochemical properties with its performance.

2. Experimental

2.1 *Catalyst preparation*

The Cu–Zn–Cr_x/Al_2O_3 catalysts were prepared by a 3-step-impregnation method. Appropriate amount of Cu $(NO_3)_2 \cdot 3H_2O$, Zn $(NO_3)_2 \cdot 6H_2O$ and Cr $(NO_3)_3$ $9H_2O$ were dissolved in 9 mL deionized water as impregnating solution. The one third solution was uniformly added drop-wise on 3 g alumina support (40–60 mesh, pre-treated at 450°C for 4 h), for 10 min, and then dried at 110°C for 20 min. Repeating above operations 2 more times, then it was dried at 110°C for 4 h and calcined at 450°C for 5 h. For the comparison, the Cu/Al_2O_3 and Cu-Zn/Al_2O_3 catalysts were prepared in the same way.

2.2 *Catalyst characterization*

The ICP-AES IRIS Advantage (TJA Solution, USA) was employed to determine the chemical compositions of the different catalyst samples by inductively coupled plasma atomic emission spectroscopy technique.

The surface area, total pore volume and average pore diameter were measured by the N_2 adsorption/desorption, using a Quantachrome Nova 1000e apparatus at liquid nitrogen temperature. Samples were degassed at 300°C for 3 h prior to analysis.

X-ray diffraction (XRD) tests were performed on DX-100 diffractometer with CuKα radiation, scanning 2θ angles in the range of 20–80°.

X-ray photoelectron spectra (XPS) were recorded with XSAM800 spectrometer with an Al$K\alpha$ (1486·6 eV) radiation.

Temperature-programmed reduction (TPR) measurements were carried out at atmospheric pressure in a fixed-bed. 50 mg sample was loaded in a quartz reactor in N_2 flow at 50°C for 30 min. Then the nitrogen was replaced by the reductive gas (5% H_2/N_2) at a flow rate of 30 mL/min. The temperature of the reactor was increased linearly from 100 to 550°C at a rate of 10°C/min by a temperature-programmed controller. The effluent stream was analysed by a thermal conductivity detector (TCD).

Cu surface area, particles size and the metal dispersion were measured by N_2O passivation method including a two-step analysis: N_2O oxidization surface Cu to Cu_2O and H_2 temperature-programmed reduction of the formed Cu_2O surface species.[22,23] A fresh 50 mg catalyst was pre-reduced at 350°C (rising the temperature at a rate of 10°C/min) for 1 h in H_2/N_2 mixture gas flow (5 vol.% at 30 mL/min). The temperature was *in situ* cooled to the adsorption temperature 60°C in pure N_2 flow (40 mL/min) and then the reduced-catalyst was exposed to the pure N_2O (30 mL/min) for 1 h to oxidize the metallic Cu to Cu_2O. After N_2O passivation, the catalyst was purged with N_2 (40 mL/min) to remove the residual oxidant and subsequently the second TPR was performed to reduce Cu_2O to Cu. The H_2 consumption in the two procedures was monitored by TCD and calculated quantitatively from the TPR peak area, calibrated with standard CuO samples.

The acidity of the calcined catalyst was characterized by temperature-programmed desorption of ammonia (NH_3-TPD) techniques. 50 mg catalyst sample, loading in the middle of quartz tube, was

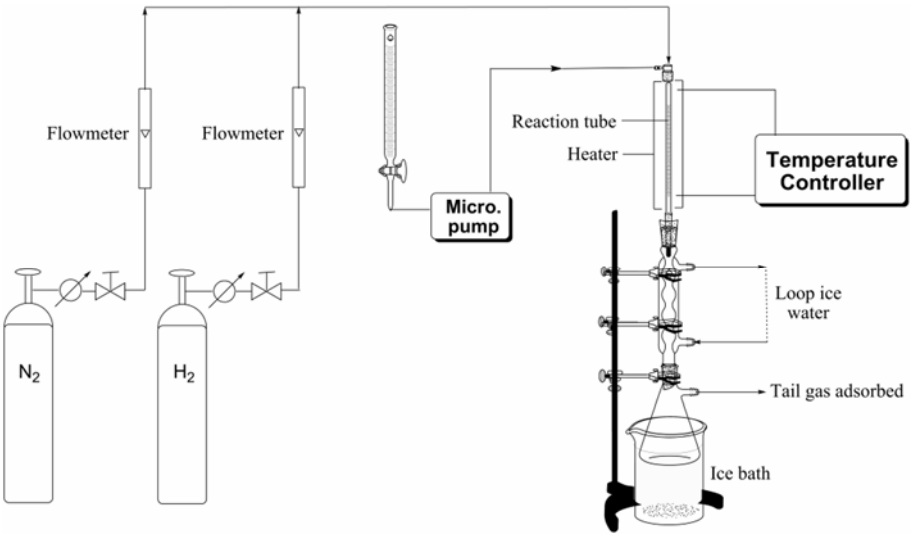

Figure 1. The reaction apparatus for synthesis of 2-methylpyrazine.

used for NH_3–TPD. Prior to analysis the sample was pre-treated *in situ* in an Ar flow (30 mL/min) at 380°C for 2 h, then cooled to the NH_3 adsorption temperature 100°C. NH_3 was absorbed by a pulsed injection in an Ar flow until saturation which was determined by the TCD signal. The TPD profiles were monitored by a thermal conductivity detector and recorded from 100 to 700°C at a heating rate of 10°C/min.

2.3 *Catalytic performance in synthesis of 2-methylpyrazine*

The catalytic activity measurements of the calcined catalysts were performed at atmospheric pressure in a continuous fixed-bed reactor (stainless steel, 8 mm i.d., 300 mm length). The reaction apparatus was showed in figure 1. The catalyst was loaded at the middle of the reaction tube with a packing height of 60 mm, reduced under the H_2 and N_2 gas mixture flow ($H_2/N_2 = 1$, molar ratio) at 380°C for 2 h and then reacted at the same temperature. The aqueous liquid reactants were prepared by mixing ethylene diamine and propylene glycol in the mole ratio of 1 : 1, and diluted with deionized water (50 wt.%). Dilution with water was helpful for reducing the viscosity and smooth feeding of the reactants. The liquid reactants were injected into the top-side of reactor by a pump at 3 mL/h and the pure nitrogen (25 mL/min) was introduced as dilute gas. The liquid products were collected in an ice-water condenser and analysed by gas chromatography (GC-112A) using a capillary column (cross-linked SE-30 gum, 0·33 mm × 30 m) and flame ionization detector (FID). The identification of the liquid products was done by GC-MS (Agligent Technol. 6890N/Agligent Technol. 5973Network Mass Selective Detector).

3. Results and discussion

3.1 *Chemical composition and the texture property*

The chemical compositions and BET data of Cu/Al_2O_3, $Cu–Zn/Al_2O_3$ and $Cu–Zn–Cr_3/Al_2O_3$ catalysts were listed in table 1. From ICP–AES results, the copper content was 11·2 wt.% for Cu/Al_2O_3 and $Cu–Zn/Al_2O_3$, 12·4 wt.% for $Cu–Zn–Cr_3/Al_2O_3$ sample. The zinc content in $Cu–Zn/Al_2O_3$ catalyst was 16·5 wt.%, and for $Cu–Zn–Cr_3/Al_2O_3$ was 16·2 wt.%. The chromium content in $Cu–Zn–Cr_3/Al_2O_3$ catalyst was 2·74 wt.%. The results of metal contents were close to those of initially calculated ones. The BET surface areas of Cu/Al_2O_3, $Cu–Zn/Al_2O_3$ and $Cu–Zn–Cr_3/Al_2O_3$ catalysts were 187·8, 126·6 and 124·7 m^2/g, respectively. A large amounts of doped Zn in Cu/Al_2O_3 resulted in the surface area decrease significantly, while only slight decrease in surface area could be found as few chromium were introduced into $Cu–Zn/Al_2O_3$ catalyst. The decrease in surface area, total pore volume and pore size indicated that not only the metallic oxide particulates were dispersed on the alumina support surface but also they could be accreted to inner wall of the pore channel.

Table 1. Compositions and textural properties of Cu/Al_2O_3, $Cu–Zn/Al_2O_3$ and $Cu–Zn–Cr/Al_2O_3$ catalysts.

Catalyst	Composition/wt. %[b]				$S_{BET}/m^2\ g^{-1}$	V/cc g^{-1}	D/nm
	Cu	Zn	Cr	Al			
Cu/Al_2O_3	11·2	–	–	47·0	187·8	0·3558	7·576
$Cu–Zn/Al_2O_3$	11·2	16·5	–	34·7	126·6	0·2312	7·416
$Cu–Zn–Cr_3/Al_2O_3$[a]	12·4	16·2	2·74	31·9	124·7	0·1984	6·269

[a]Chromium initial calculated content is 3 wt.%. [b]calculated from ICP-AES

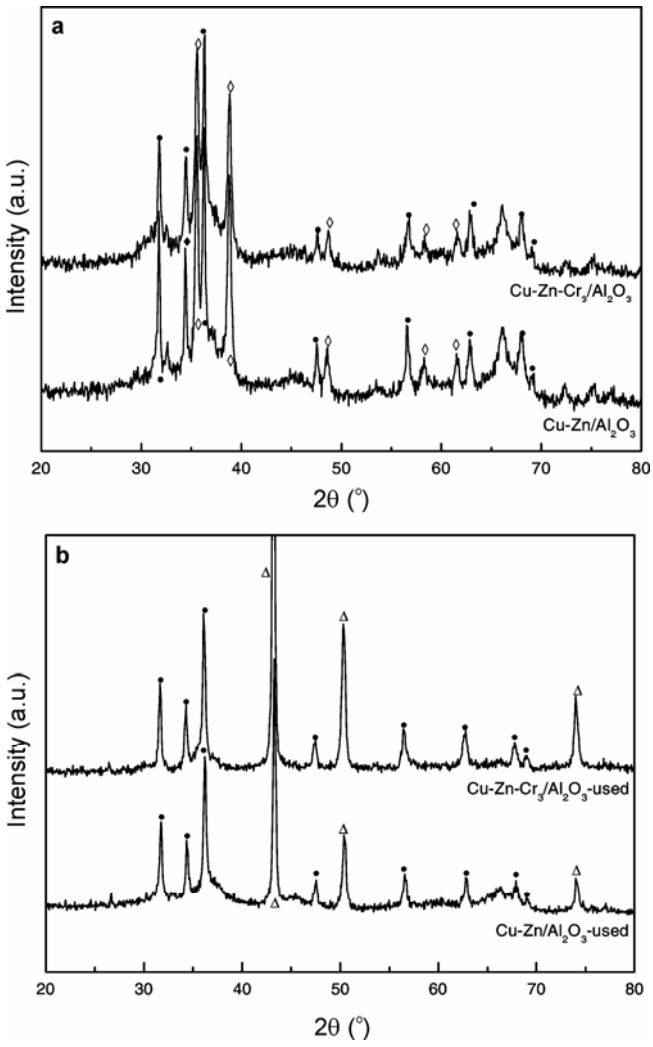

Figure 2. **a**, XRD patterns of fresh $Cu–Zn/Al_2O_3$ and $Cu–Zn–Cr_3/Al_2O_3$ catalysts. **b**, XRD patterns of used $Cu–Zn/Al_2O_3$ and $Cu–Zn–Cr_3/Al_2O_3$ catalysts.

3.2 *Phase composition of the catalyst*

XRD analysis was employed to investigate the crystal of the elements of the catalyst samples, and the XRD patterns of the fresh catalysts and used catalysts were obtained (see figures 2a and b). Both patterns of two fresh catalyst samples revealed highly characteristic reflection of ZnO and CuO. While the chromium species, generally existing as spinel in Cr rich Cu-Zn-Cr catalytic system,[24–26] had very weak intensity, which probably could explain that the amorphous chromium species existed in the catalyst with low chromium content.

Figure 2b showed XRD patterns of used $Cu–Zn/Al_2O_3$ and $Cu–Zn–Cr_3/Al_2O_3$ catalysts. For $Cu–Zn/Al_2O_3$ catalyst, the diffraction peaks of metallic copper phase were observed as the effect of pre-reduction with H_2 and ZnO could not be reduced. As to be expected, there was no obvious diffraction peak of chromium species because of its possible amorphous state in $Cu–Zn–Cr_3/Al_2O_3$ catalyst, which may be enhanced by H_2 pre-treatment.

3.3 *Chemical state of the surface elements by XPS*

The surface analysis of the catalysts and the chemical state of the elements were evaluated by XPS technique, the catalyst samples were pre-treated by using hydrogen gas at 380°C for 2 h prior to analysis. The XPS spectra of the $Cu2p_{3/2}$ of $Cu–Zn/Al_2O_3$ and $Cu–Zn–Cr_3/Al_2O_3$ catalysts were shown in figure 3. The copper oxide displayed strong shake-up peak near 935·0 eV, which is the characteristic of Cu^{2+} species. Another means of identifying Cu^{2+} cation was the satellite peak, about 8 eV on the high binding energy side, due to the shake-up transition by ligand → metal 3*d* charge transfer, which cannot occur in Cu^+ and Cu^0 because of their fully filled 3*d* shell.[27–29] The peaks around 932·4 eV were assigned to the cuprous cations and/or metallic copper.[30] In the XPS spectrum of $Cu–Zn–Cr_3/Al_2O_3$ catalyst, the Cu^{2+} species with considerable peak intensity were detected, because the reduced sample was exposed to air before XPS examination, the detected amounts of copper species in the sample did not characterize the surface composition of the catalyst under the reaction conditions. Instead, these data illustrated partial reoxidation of the catalyst when the sample

conditioned in reaction environment was exposed to air at room temperature.[31] This low-temperature reoxidation apparently affected only a thin surface layer, because XRD analysis did not detect copper oxides in the reduced sample. The XPS analysis results suggested that the metallic copper content increased significantly on the catalyst surface and the introduction of chromium enhanced the reduction compared to the catalyst without chromium.

3.4 *The reducibility for the catalyst*

The TPR profiles of Cu/Al_2O_3, $Cu–Zn/Al_2O_3$ and $Cu–Zn–Cr_3/Al_2O_3$ catalysts were presented in figure 4. It was shown that the Cu/Al_2O_3 catalyst had two reduction peaks detected at 251 and 297°C, which could be assigned to $Cu^{2+} \rightarrow Cu^{+}$ and $Cu^{+} \rightarrow Cu^{0}$.[32] Two similar TPR patterns, different from that of Cu/Al_2O_3 catalyst, were observed in $Cu–Zn/Al_2O_3$ and $Cu–Zn–Cr_3/Al_2O_3$ catalysts with only one reduction peak assigned the reduction of Cu^{2+} direct to Cu^{0} under different reduction temperatures.

The reduction peak area was in proportion to the reducible copper content for the copper-based catalyst. The variation of reduction peak area indicated that the catalyst reducibility was modified by the addition of promoter. From the results of the quantitative calculation, the $Cu–Zn–Cr_3/Al_2O_3$ catalyst sample displayed the higher peak area than that of $Cu–Zn/Al_2O_3$ catalyst, corresponding to larger amounts of hydrogen consumption, which suggested that more copper oxides were enriched on the catalyst surface. The reduction temperature shifted to lower temperature side also indicated that the Cu^{2+} species were easily reduced to lower valency species by promotion of chromium.[33–36] As a result, larger number of metallic Cu could be reduced, corresponding to larger peak intensity and peak area proportion of metallic Cu in XPS spectra.

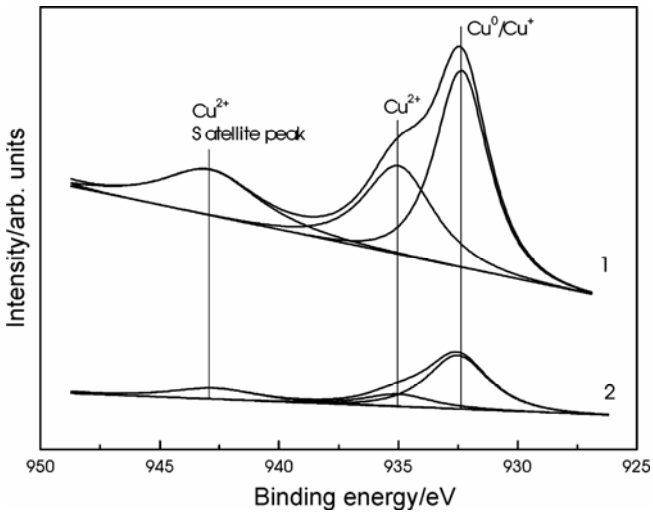

Figure 3. XPS spectra of $Cu–Zn/Al_2O_3$ and $Cu–Zn–Cr_3/Al_2O_3$ catalysts.

3.5 *Cu surface area, dispersion and Cu/CuO crystallite size*

Cu surface area and dispersion, are important parameters for Cu-based catalyst, are generally obtained by N_2O chemisorption.[37,38] Copper dispersion (D_{Cu}), defined as the ratio of Cu exposed at the surface to total, was calculated from the amount of H_2 consumed in the TPR process of $Cu_2O \rightarrow Cu$. Starting from the D_{Cu} value, Cu metal surface area (MSA) was calculated.[39]

$$\mathrm{MSA}\ (\mathrm{m^2 g_{Cu}^{-1}}) = \frac{\mathrm{Mol_{H_2}} \cdot \mathrm{SF} \cdot N_A}{10^4 \cdot \mathrm{C_M} \cdot \mathrm{W_{Cu}}},$$

where Mol_{H_2}, SF, N_A, C_M and W_{Cu} are moles of hydrogen experimentally consumed per unit mass of catalyst ($\mu mol_{H_2} g^{-1}{}_{cat}$), stoichiometric factor (2), Avogadro's number ($6{\cdot}022 \times 10^{23}$ mol^{-1}), number of surface Cu atoms per unit surface area ($1{\cdot}47 \times 10^{19}$ atoms m^{-2}), and Cu content (wt.%), respectively. The O/Cu ratio is assumed to be 1/2 (SF = 2) on the basis of UPS results,[39] which proved that after oxidation with N_2O at temperatures up to 100–120°C,

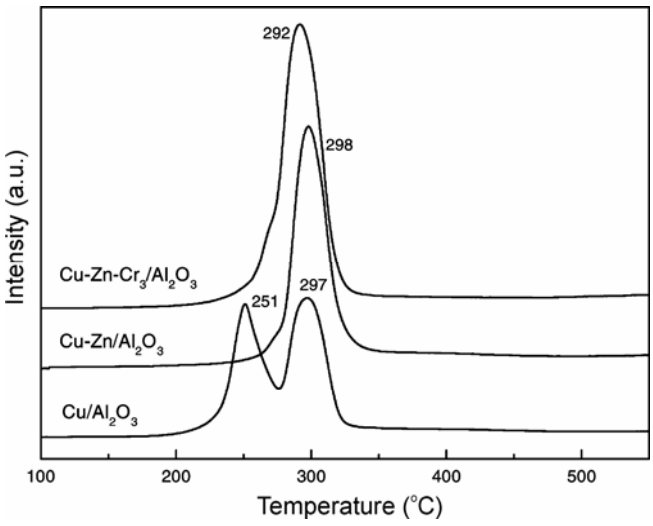

Figure 4. TPR profiles of Cu/Al_2O_3, $Cu–Zn/Al_2O_3$ and $Cu–Zn–Cr_3/Al_2O_3$ catalysts. The chromium initial calculated content was 3 wt.% in $Cu–Zn–Cr_3/Al_2O_3$ catalyst.

Table 2. Surface characteristics of dispersed copper catalysts.

	TPR–N_2O passivation method			
Catalyst	Surface Cu content (μmol/g_{cat})	Mol_{H2} (μmol/g_{cat})	MSA (m^2/g_{Cu})	D_{Cu} (%)
Cu–Zn/Al_2O_3	8·0	4·0	183·1	28·4
Cu–Zn–Cr_3/Al_2O_3	12·2	21·9	358·8	55·7

Table 3. Crystallite size variation via H_2 treatment for Cu–Zn/Al_2O_3 and Cu–Zn–Cr_3/Al_2O_3 samples.

Catalyst	CuO (202) [nm]	Cu (200) [nm]
Cu–Zn/Al_2O_3	31·0	–
Cu–Zn–Cr_3/Al_2O_3	31·2	–
Cu–Zn/Al_2O_3 used	–	28·8
Cu–Zn–Cr_3/Al_2O_3 used	–	27·0

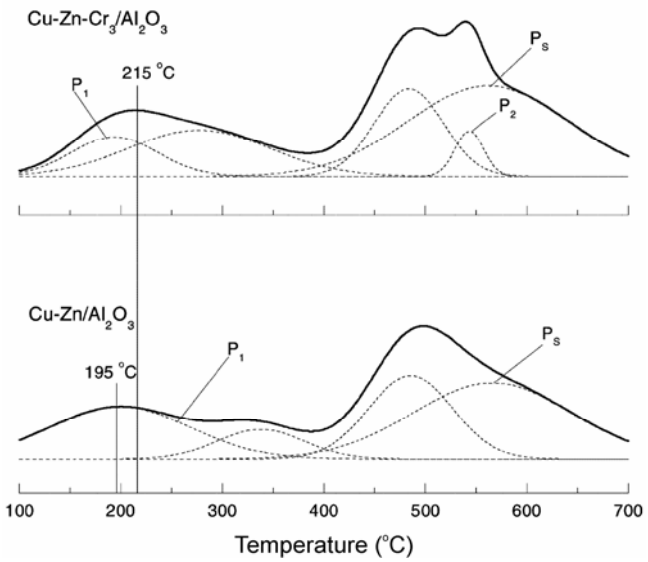

Figure 5. NH_3-TPD curves for Cu–Zn/Al_2O_3 and Cu–Zn–Cr_3/Al_2O_3 samples. The TPD curves were deconvolved using a Gaussian shaped function. The solid lines are the TPD curves and the dashed lines are the fitting curves.

the surface copper is primarily in the Cu^+ oxidation state. The results from N_2O chemisorption were summarized in table 2. It was shown that the Cr-promoted Cu–Zn/Al_2O_3 displayed larger value of surface Cu content, corresponding to larger amount of H_2 consumption and Cu surface area (MSA) which increased by almost 1 time. So did the Cu dispersion.

The crystallite size of CuO and Cu may be estimated from the values of the full-width at half-maximum (FWHM) of the (202) and (200) diffraction peaks by means of the Scherrer equation $L = 0{\cdot}89\lambda/\beta(\theta)\cos\theta$, where L is the crystallite size, λ is the wavelength of the radiation used, θ is the Bragg diffraction angle, and $\beta(\theta)$ is the FWHM.[40] The results are given in table 3. For the fresh samples, the crystallite size value of CuO of Cu–Zn–Cr_3/Al_2O_3 catalyst was slightly bigger than that of Cu–Zn/Al_2O_3 catalyst, which may be responsible for the decrease to a small extent in surface area as described in table 1. The CuO phases were reduced to metallic Cu in H_2 gas flow under the reaction conditions, the crystallite size values decreased by 7·10% and 13·46% for Cu–Zn/Al_2O_3-used and Cu–Zn–Cr_3/Al_2O_3-used samples, respectively. It was suggested that the reducibility of Cu–Zn/Al_2O_3 catalyst was improved significantly by adding chromium promoter, the smaller Cu particles generated larger metallic Cu surface area and dispersion, resulting in the Cu particles enriched on the catalyst surface but no sintering.[31]

3.6 *The amount of acid sites and acid strength distribution of the catalyst*

NH_3–TPD analysis was carried out in order to investigate the amount of acid sites and acid strength distribution, the TPD curves were depicted in figure 5 and the details were reported in table 4. In the both TPD curves, four desorption regions of 100–300°C, 300–400°C, 400–590°C and 590–700°C, were observed. The desorption peak below 300°C was not ascribed to the ammonia directly adsorbed on the acid sites but for possible ammonia molecules interaction with the terminal OH groups on the catalyst surface, which were desorbed easily on the TPD test (this process was denoted as P_1 in figure 5).[41,42] The high-temperature peaks (400–590°C) were assigned to desorption of NH_3 from the strong acid sites.[43] The difference between the TPD curves for Cu–Zn/Al_2O_3 and Cu–Zn–Cr_3/Al_2O_3 catalysts was found, it was single peak for that of Cu–Zn/Al_2O_3 while it was double peaks for that of Cu–Zn–

Table 4. Acid strength distribution for $Cu–Zn/Al_2O_3$ and $Cu–Zn–Cr_3/Al_2O_3$ catalysts and their catalytic performances for 2-MP synthesis.

	Acidity (NH_3 uptake, mmol/g)					
Catalyst	100–300	300–400	400–590	590–700°C	Total acidity	2-MP selectivity (%)
$Cu–Zn/Al_2O_3$	0·78	0·21	2·37	0·48	3·84	68·0
$Cu–Zn–Cr_3/Al_2O_3$	1·08	0·12	2·41	0·42	4·03	84·8

Table 5. Effect of chromium content on synthesis of 2-methylpyrazine.

			Selectivity (%)					
Catalyst	ED conv.	PG conv.	Lb	Py	2-MP	2-MPIP	Alkyl pyrazines	Others
Cu/Al_2O_3	76·7	80·2	11·0	14·79	53·35	5·02	14·01	1·83
$Cu–Zn/Al_2O_3$	88·1	90·5	2·82	21·47	68·02	4·26	2·06	1·38
$Cu–Zn–Cr_1/Al_2O_3$	93·6	96·1	3·65	10·58	81·46	2·23	0·82	1·25
$Cu–Zn–Cr_3/Al_2O_3$	97·9	100	3·43	6·99	84·75	2·42	1·01	1·40
$Cu–Zn–Cr_5/Al_2O_3$	95·7	98·7	3·32	6·59	84·64	3·04	1·04	1·37
$Cu–Zn–Cr_7/Al_2O_3$	95·4	98·2	3·08	8·17	82·62	2·86	1·37	1·90

ED = ethylene diamine, PG = propylene glycol, Lb = lower boiling point components, Py = pyrazine, 2-MP = 2-methylpyrazine, 2-MPIP = 2-methylpiperazine. Reaction conditions: atmosphere, temperature = 380°C, time on stream = 2 h, LHSV = 1 h^{-1}, ED : PG = 1 : 1 (mol) in 50 wt.% aq. solution

Cr_3/Al_2O_3 catalyst. The overlapped peaks indicated that there might be stronger acid sites (denoted as P_2) in $Cu–Zn–Cr_3/Al_2O_3$ sample, the deconvolution indeed showed that there were two different strength acid sites with different desorption temperature. The each TPD curve displayed a broadening shoulder peak (denoted as P_s) around 600°C, corresponding to the formation of strongly Lewis acid sites generated by Zn^{2+}, which was identified that the low-temperature peak (100–300°C) was widened and shifted to high-temperature side.[17,44,45] Cu-Zn-Cr_3/Al_2O_3 showed an increase of NH_3 desorption from 0·78 to 1·08 mmol/g compared to Cu-Zn/Al_2O_3 (table 4). The total acidity also increased by 4·9%. It was shown that the increased acidity displayed a considerable effect on the catalytic performance, the selectivity of 2-MP increased by 24·7%.

3.7 *Catalytic synthesis of 2-methylpyrazine from ED and PG*

3.7a *Effect of chromium content on catalytic performance:* The effects of $Cu–Zn/Al_2O_3$ catalyst promoted by chromium of different concentration on the conversions of reactants and the products selectivities were studied and the results were summarized in table 5. It is clear from the table that the catalysts containing chromium produced less amount of pyrazine, alkyl pyrazine and intermediate product, 2-methylpiperazine as compared with those of the catalysts without chromium. The selectivity of 2-methylpyrazine increased to 84·75% over $Cu–Zn–Cr_3/Al_2O_3$ catalyst compared to 68·02% on $Cu–Zn/Al_2O_3$ catalyst. Keeping the copper and zinc concentration constant, 15 wt.% and 20 wt.% respectively, the effects of different chromium concentration were studied at the same conditions, and the results showed that the optimum concentration of chromium was 3 wt.%. The results of BET revealed that chromium promoted the dispersion of active copper species and acted as a fence to separate active species from congregating, addition of chromium promoter was helpful for dehydration-cyclization and dehydrogenation of ethylene diamine and propylene glycol to 2-methylpyrazine. Further studies were carried out over $Cu–Zn–Cr_3/Al_2O_3$ catalyst, as it showed good conversion of ethylene diamine and propylene glycol and selectivity of 2-methylpyrazine.

3.7b *Influence of reaction temperature:* Figure 6 showed that the effect of reaction temperature on reactants conversions and products distribution, the reaction was preformed over $Cu–Zn–Cr_3/Al_2O_3$ catalyst for 2 h time on stream at a LHSV of 1 h^{-1}. The

ethylene diamine conversion increased with the reaction temperature from 87·5% at 340°C to 98·1% at 420°C. The selectivity of 2-methylpyrazine was up to maximum 83·12% at 380°C. Only a small amount of lower boiling point components was detected in products, whose concentration was higher at lower reaction temperature (340°C) compared with higher reaction temperature. At higher reaction temperature, the lower boiling point components like methanol and acetaldehyde were readily reacting with piperazine and pyrazine, giving alkyl pyrazine, which resulted in decreasing slightly in concentration of lower boiling point components rather than higher to be expected. Besides, the piperazine ring structure could be easily cracked at higher reaction temperature with the concurrent formation of side reaction products and ammonia,[18] which also reacted with pyrazine and 2-methylpyrazine to alkyl pyrazine. As a result, the selectivities of pyrazine, 2-methylpyrazine and 2-methylpiperazine decreased, in contrast to increased of alkyl pyrazine.

3.7c *Product distribution versus molar ratio of reactants:* A series of experiments were performed to determine the optimum feed ratio at 380°C with different mole ratio of ethylene diamine and propylene glycol over Cu–Zn–Cr_3/Al_2O_3 catalyst and the results were presented in table 6. It could be found from the table that the ethylene diamine conversion decreased when the mole ratio of ethylene diamine increased. The concentration of pyrazine increased from 6·69 to 13·6% with the mole ratio from 1 to 1·5, which was probably contributed to the self-cyclocondensation of ethylene diamine. The selectivity of 2-methylpyrazine decreased as ethylene diamine concentration increasing in the feed. It could also be noted that the formation of 2-methylpiperazine, which was the primary intermediate product, which had the same trend with 2-methylpyrazine.

3.7d *Role of LHSV in synthesis of 2-methylpyrazine:* It was demonstrated that the effect of liquid hourly space velocity (LHSV) on the formation of 2-methylpyrazine in figure 7. It is clear that the conversions of the reactants as well as selectivity for 2-methylpyrazine decreases with increase in LHSV. However, the increase in selectivity of 2-methylpiperazine, the main intermediate product, indicated that dehydrogenation had not been well performed due to the less contact time. At low LHSV, 2-methylpyrazine and pyrazine were the major products. As LHSV increased from 1 h^{-1} to 2·4 h^{-1}, the selectivity of 2-methylpyrazine decreased from 83·1 to 65·0%, that of alkyl pyrazines increased resulting from dehydrogenation of pyrazine, piperazine and their methyl derivative and alkylation of that with the lower boiling point components like acetone, lower alcohols and acetaldehyde, which were easily formed at a high LHSV value.

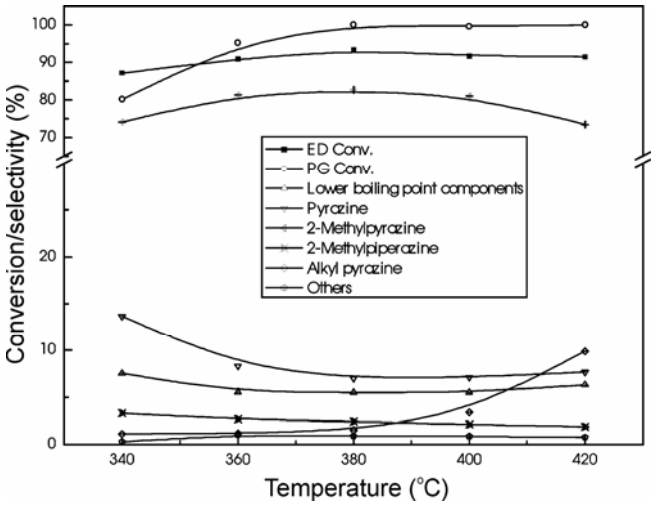

Figure 6. Influence of temperature on synthesis of 2-methylpyrazine over Cu–Zn–Cr_3/Al_2O_3 catalyst. Reaction conditions: atmospheric, time on stream = 2 h, LHSV = 1 h^{-1}, ED: PG = 1 : 1 (mol) in 50 wt.% aq. solution.

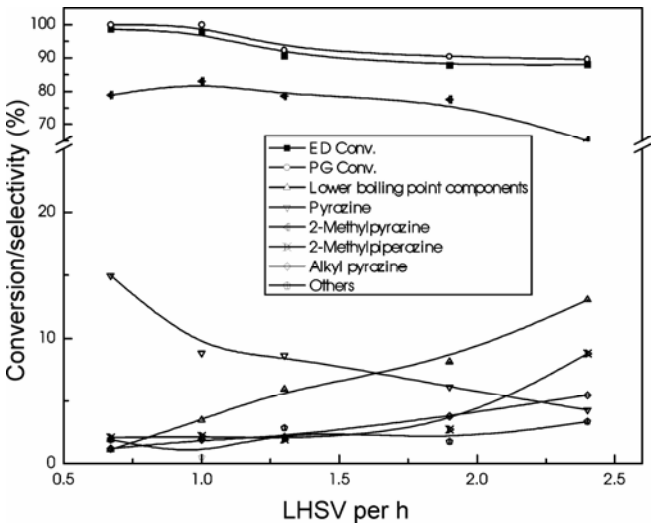

Figure 7. Influence of LHSV on synthesis of 2-methylpyrazine over Cu–Zn–Cr_3/Al_2O_3 catalyst. Reaction conditions: atmosphere, temperature = 380°C, time on stream = 2 h, ED : PG = 1 : 1 (mol) in 50 wt.% aq. solution.

Table 6. Effect of molar ratio of ethylene diamine and propylene glycol on synthesis of 2-methylpyrazine over Cu–Zn–Cr_3/Al_2O_3 catalyst.

			Selectivity (%)					
Molar ratio ED : PG	ED conv.	PG conv.	Lb	Py	2-MP	2-MPIP	Alkyl pyrazines	Others
1 : 1·5	100·0	95·2	5·27	2·54	85·88	2·81	1·76	1·76
1 : 1.2	98·5	98·8	2·96	5·21	86·26	2·73	1·66	1·20
1 : 1	97·9	100·0	3·47	6·87	85·09	2·18	1·89	0·49
1·2 : 1	92·4	97·5	3·59	8·19	82·24	2·26	3·09	0·64
1·5 : 1	79·8	97·1	3·99	13·64	75·71	1·84	4·05	0·78

ED = ethylene diamine, PG = propylene glycol, Lb = lower boiling point components, Py = pyrazine, 2-MP = 2-methylpyrazine, 2-MPIP = 2-methylpiperazine. Reaction conditions: atmosphere, temperature = 380°C, time on stream=2 h, LHSV = 1 h^{-1}, water = 50 wt.% in the reactants.

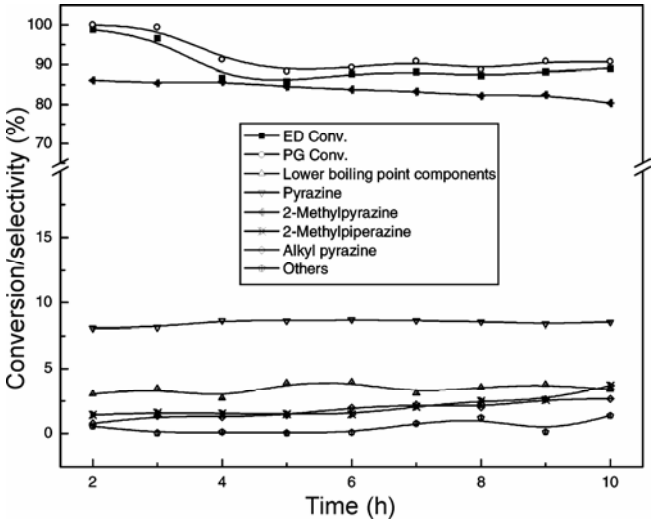

Figure 8. Influence of time on synthesis of 2-methylpyrazine over Cu–Zn–Cr_3/Al_2O_3 catalyst. Reaction conditions: atmosphere, temperature = 380°C, LHSV = 1 h^{-1}, ED : PG = 1 : 1 (mol) in 50 wt.% aq. solution.

3.7e *Relationship between catalytic activity and time on stream:* The stability was investigated over Cu–Zn–Cr_3/Al_2O_3 catalyst for 10 h (see figure 8). Initially, the deactivation was faster, the conversion of ethylene diamine dropped sharply from 97·9 to 90% in 4 h and kept constant till the end (10 h). The selectivity of 2-methylpyrazine decreased from 86·2 to 80·3%, that of 2-methylpyrazine and pyrazine was over 90%. At the end of the period of this run, the selectivity of 2-methylpiperazine increased to a little extent, which indicated that dehydrogenation was weakened. The results showed the high activity of composite catalyst in conversion of ethylene diamine and high selectivity and stability of 2-methylpyrazine.

Conclusions

The novel Cr-modified Cu–Zn/Al_2O_3 catalysts were prepared by a 3-step impregnation method. The N_2 adsorption/desorption tests showed that the addition of chromium had little effect on the surface area and pore diameter, only evident changes were observed in pore volume. Considering the influences of chromium on the catalytic performance, the better catalytic activity (selectivity of 2-MP > 80%) and reaction stability could be obtained compared with those of the samples without chromium. It suggested that chromium acted the role of structure promoter. XRD results suggested that chromium species might exist in catalyst as amorphous state. The dispersion of active site Cu increased by almost 1 time and the total acidity was significantly improved by 4·7% after of addition chromium promoter; furthermore, catalytic activity was improved. The chromium promoted catalyst displayed better reducibility compared to the catalyst without chromium according to the results of XPS, N_2O chemisorption and TPR measurements.

The catalytic activity for 2-methylpyrazine synthesis by cyclo-dehydrogenation of ethylene diamine and propylene glycol was carried out at 380°C over the chromium-promoted Cu–Zn/Al_2O_3 catalysts. The Cu–Zn–Cr_3/Al_2O_3 catalyst has shown good conversions of reactants, high selectivity and excellent stability of 2-methylpyrazine after reacting for 10 h. The optimum chromium content was 3 wt.%.

Acknowledgements

The authors wish to thank the Analysis and Test Centre of Sichuan University for ICP-AES test. Thanks are also due to Fang Guo, Fenfen Qu and Jinyan Hu for useful discussion.

References

1. Cenker M, Trenton and Baxter G E 1961 US 3005820
2. Su W Y and Knifton J F 1988 US 4788289
3. Subrahmanyam, M, Kulkarni S J and Rao A V R 1995 *Indian J. Chem. Technol*. **2** 237
4. Seetharamanjaneya S P, Raghavan K V, Rao P K and Kulkarni S J 2002 US 143180 A1
5. Forni L, Stern G and Gatti M 1987 *Appl. Catal.* **29** 161
6. Subrahmanyam M, Muralidhar G and Kulkarni S J 2000 IN 185171
7. Forni L and Pollesel P 1991 *J. Catal.* **130** 403
8. Sato K 1978 US 4097478
9. Subrahmanyam M, Muralidhar G and Verma P K 2001 IN 185482
10. Lee Y K, Park S E and Kwon Y S 1990 US 4966970
11. Shoji T, Nakaishi T and Mikata M 1996 JP 08225543A
12. Balpanov D S, Krichevskii L A and Kagarlitskii A D 2001 *Russ. J. Appl. Chem.* **74** 2125
13. Fedolyak G T, Morozov A V, Kagarlitskii A D, Krichevskii L A and Akad I 1990 *Nauk Kaz. SSR, Ser. Khim.* **6** 85
14. Shoji T and Nakaishi T 1997 US 5693806
15. Forni L and Nestori S 1998 *Stud. Surf. Sci. Catal.* **41** 291
16. Anand R and Rao B S 2002 *Catal. Commun.* **3** 29
17. Anand R, Hegde S G, Rao B S and Gopinath C S 2002 *Catal. Lett.* **84** 265
18. Dixon J K 1946 US 2400398
19. Pfann H F, Greenwich and Dixon J K 1947 US 2414552
20. Park I, Lee J, Rhee Y, Han Y and Kim H 2003 *Appl. Catal. A: Gen* **253** 249
21. Park I, Rhee Y, Lee J, Han Y H, Jeon J and Kim H 2003 *Res. Chem. Intermed.* **29** 575
22. Cesar D V, Perez C A, Salim V M M and Schmal M 1999 *Appl. Catal. A: Gen* **176** 205
23. Velu S, Suzuki K and Osaki T 1999 *Catal. Lett.* **62** 159
24. Lindstrom B, Pettersson L J and Menon P G 2002 *Appl. Catal. A: Gen.* **234** 111
25. Fujiwara M, Kieffer R, Ando H and Souma Y 1995 *Appl. Catal. A: Gen.* **121** 113
26. Fujiwara M, Ando H, Tanaka M and Souma Y 1995 *Appl. Catal. A: Gen.* **130** 105
27. Murcia-Mascaros S, Navarro R M, Gomez-Sainero L and Fierro J L G 2001 *J. Catal.* **198** 338
28. Diaz G, Perez-Hernandez R, Gomez-Cortes A, Benaissa M, Mariscal R and Fierro J L G 1999 *J. Catal.* **187** 1
29. Campos-Martin J M, Guerrero-Ruiz A and Fierro J L G 1995 *J. Catal.* **156** 208
30. Mathew T, Rao B S and Gopinath C S 2004 *J. Catal.* **222** 107
31. Ilinich O, Ruettinger W, Liu X S and Farrauto R 2007 *J. Catal.* **247** 112
32. Zhai X, Shamoto J, Xie H and Han Y 2008 *Fuel* **87** 430
33. Tan Y, Xie H, Cui H and Han Y 2005 *Catal. Today* **104** 25
34. Chen C S, Cheng W H and Lin S S 2003 *Appl. Catal. A: Gen.* **238** 55
35. Huang L H, Chu W, Long Y, Ci Z M and Luo S Z 2006 *Catal. Lett.* **108** 113
36. Chu W, Zhang T, He C H and Wu Y T 2002 *Catal. Lett.* **79** 129
37. Guerreiro E D, Gorriz O F, Larsen G and Arrua L A 2000 *Appl. Catal. A: Gen* **204** 33
38. Turco M, Bagnasco G, Cammarano C, Senese P, Costantino U and Sisani M 2007 *Appl. Catal. B: Environ.* **77** 46
39. Gervasini A and Bennici S 2005 *Appl. Catal. A: Gen* **281** 199
40. Zhao Y, Li F, Zhang R, Evans D G and Duan X 2002 *Chem. Mater.* **14** 4286
41. Mathew T, Vijayaraj M, Pal S, Tope B B, Hegde S G, Rao B S and Gopinath C S 2004 *J. Catal.* **227** 175
42. Mathew T, Tope B B, Shiju N R, Hegde S G, Rao B S and Gopinath C S 2002 *PCCP* **4** 4260
43. Barthos R, Lonyi F, Onyestyak G and Valyon J 2001 *Solid State Ionics* **141** 253
44. Katada N, Endo J, Notsu K, Yasunobu N, Naito N and Niwa M 2000 *J. Phys. Chem.* **B104** 10321
45. Roessner F, Hagen A, Mroczek U, Karge H G and Steinberg K H 1993 *Stud. Surf. Sci. Catal.* **B75** 1707